ChemPubSoc Europe

DOI: 10.1002/ejic.201801539

EurJIC European Journal of Inorganic Chemistry

Full Paper

Nanoparticles for Drug Delivery

Nanoplatforms of Manganese Ferrite Nanoparticles Functionalized with Anti-Inflammatory Drugs

Kleoniki Giannousi,[a] Emmanouil Koutroumpis,[a] Violetta Georgiadou,[a] Vasilis Karagkounis,[a] and Catherine Dendrinou-Samara*[a]

Abstract: Targeted drug delivery by magnetic nanoparticles (MNPs) is at the leading edge of the rapidly developed methods for the diagnosis and treatment of various diseases. Functionalization of nonsteroidal anti-inflammatory drugs (NSAIDs) onto MNP-based platforms constitutes a challenging endeavor, as it is based on the physicochemical characteristics of the final carrier/system. $MnFe_2O_4$ MNPs of relatively small size and enhanced magnetization with aminated (AmMNPs) and non-aminated (Non-AmMNPs) surface were prepared solvothermally in the presence of octadecylamine(ODA) through synthetic variations. Three nonsteroidal anti-inflammatory drugs (NSAIDs), acetylsalicylic acid (ASA), mefenamic acid (MEF) and Naproxen (NAP), of different pharmacochemical properties, were used for the loading of the nanoplatforms. In the case of AmMNPs, attachment of the NSAIDs was achieved by direct coupling of carboxylate donors with the NH_2 groups via the formation of an amide bond, whereas indirect coupling of the drugs through encapsulation was applied on Non-AmMNPs by taking advantage of the PEGylation approach. FT-IR and UV/Vis data confirmed the distinct drug release behavior, which is attributed to different cross-linking forces depending on the method of functionalization. The biological behavior and anti-inflammatory activity of the MNPs@NSAIDs was evaluated in vitro; AmMNPs@ASA inhibited lipoxygenase (LOX) and protected albumin denaturation with values comparable with those of NSAIDs.

1. Introduction

Nonsteroidal anti-inflammatory drugs (NSAIDs) are a wide group of cyclooxygenase (COX) inhibitors that work by blocking the production of prostaglandins (PGs), albeit with side effects, such as stomach irritation, ulcers and renal toxicity.[1] Recent epidemiological studies correlate the prolonged usage of NSAIDs with slowing the progression of Alzheimer's Disease (AD).[2] However, the potential of NSAIDs for the treatment of AD are correlated with a number of factors, e.g. the physicochemical characteristics, brain penetration properties and dosage of the drugs. Conventional analgesic NSAIDs include acetylsalicylic acid (ASA),[3] mefenamic acid (MEF)[4,5] and naproxen (NAP).[6,7] NSAIDs are widely administered against a wide range of inflammatory diseases to treat moderate pain including fever, headache, dental pain, postoperative and postpartum pain, dysmenorrhea, osteoarthritis, rheumatoid arthritis.[3–7] However, NSAIDs are accompanied with limitations such as lack of specificity toward desired tissues, high distribution volume, lack of selectivity, poor aqueous solubility and dissolution rate. Controlled drug release systems could overcome the above-mentioned drawbacks, since they result to lower doses of active agent, due to preservation of the drugs by simultaneously avoiding their destruction.[8,9]

Magnetic nanoparticles (MNPs) based drug delivery platforms have been proposed as suitable vehicles for overcoming pharmacokinetic limitations associated with conventional drug formulations.[10] Considering also the heterogeneity of enhanced permeability and retention (EPR) effect, magnetic targeting boosts the accumulation of MNPs in the diseased area.[11] However, biological barriers not only affect the movement of MNPs, but also alter their magnetic and surface properties and/or induce a negative host response through biochemical signaling, resulting in an early uptake by cells before the MNPs manage to reach the target tissue.[12] Nonetheless, appropriate functionalization of the MNPs could result in the design of multifunctional drug carriers, finding applications as contrast agents in magnetic resonance imaging and/or in magnetic hyperthermia.[13,14] Even though polymeric nanoparticles and MNPs have been studied in the area of theranostics in the sense that diagnosis coexists with targeted drug and/or gene delivery in case of tumors,[3–8,15] the use of MNPs as NSAIDs carriers has been scarcely reported.[16]

Recently, manganese ferrite ($MnFe_2O_4$) nanoparticles due to their unique properties have been the subject of extensive research, concerning multiple functionalities of catalysis, adsorbent, water treatment, imaging, hyperthermia and triggered drug release.[17] $MnFe_2O_4$ MNPs show greater biocompatibility, have high magnetization, large relaxivity and a strong T_2 phase contrast for magnetic resonance imaging compared to Fe_3O_4,

[a] *Laboratory of Inorganic Chemistry, Department of Chemistry, Aristotle University of Thessaloniki, Thessaloniki, 54124 Greece*
E-mail: samkat@chem.auth.gr
http://users.auth.gr/samkat

Supporting information and ORCID(s) from the author(s) for this article are available on the WWW under https://doi.org/10.1002/ejic.201801539.

γ-Fe_2O_3, $CoFe_2O_4$, and $NiFe_2O_4$ MNPs.[18] Interestingly, it has been reported that suitable surface modification onto the nanoparticles not only can prevent aggregation and clustering, but also results to prolonged circulation in the blood vessels, since NPs are being less recognized by the reticulo-endothelial system (RES).[12]

The prerequisites for using MNPs in bio-applications are multifaceted and include specific physicochemical characteristics (size, shape, structure and surface chemistry known as 4S's) and magnetic properties, which lead to desirable biodistribution, image contrast, target selectivity and sustained drug release. The successful preparation of primary nanoparticles with desired characteristics is nowadays the preliminary step for moving forward to the next generation of secondary nanomaterials, which can be designed via appropriate synthetic and/or post-synthetic functionalization of the primary MNPs. An ultimate rational way that such systems can be formed is missing, due to the fact that each drug possesses its unique physicochemical characteristics. In so, direct and indirect methods of functionalization have emerged. As far as direct conjugation concerned, coupling with reactive functional groups such as a primary or a secondary amino, carboxyl, hydroxyl, alkyl halogen, or azide are in practice.[19] On the other hand, indirect drug loading has also been studied through intermediate biocompatible coatings e.g. Polyethylene glycol (PEG) polymers, Polyethyleneimine (PEI) molecules, dextranes, liposomes, chitosan etc. that offer excellent chemical stability, precise control over composition and structure and hence high efficiency in biomedical applications but suffers from the final size;[12,20] when the size increases, more NPs are entrapped within the liver and spleen.[10,11]

Herein, we propose a simple synthetic variation which allows the preparation of octadecylamine (ODA) coated manganese ferrite magnetic nanoparticles ($MnFe_2O_4$ MNPs) either with aminated (AmMNPs) or non-aminated (Non-AmMNPs) groups on their surface. During synthesis, when octadecylamine (ODA) has been used in a triple role (coating, solvent, reducing agent) AmMNPs have been isolated, while in the presence of a non-polar solvent (diphenyl ether, DPE) Non-AmMNPs have been produced. The resulted MNPs were functionalized through post-synthetic procedures with three NSAIDs of different molecular weight and structure with a common feature of carboxylate donor; ASA, MEF and NAP. By taking into account that different inflammation-related diseases require different drug administration routes, we aimed at unique release profiles. The functionalization of the MNPs with the drugs aimed at confining the side-effects and giving them a specific delivery profile. For example, in the long-term treatment of rheumatoid arthritis, osteoarthritis and ankylosing spondylitis, the transdermal topical route is preferable with initial burst drug release followed by a second slow release.[21] For that purpose, two procedures were employed for the transformation of the synthesized $MnFe_2O_4$ MNPs as carriers: (i) an amide reaction through the carboxylate donor of the drugs with the AmMNPs (direct coupling) and (ii) loading of the drug on the PEG matrix of the Non-AmMNPs MNPs (indirect coupling). The nanoplatforms were examined as anti-inflammatory agents by evaluating in vitro the inhibition of the enzymatic activity of lipoxygenase (LOX) and the protection of albumin denaturation, with NSAIDs as the standard reference drugs.

2. Results and Discussion

2.1. Synthetic Aspects, Characterization, and Functionalization of MNPs

We have shown before that based on the synthetic conditions, the linear configuration of ODA molecules can lead to unshielded NH_2 groups on the surface of $CoFe_2O_4$ MNPs.[22] In the present study we tested if this efficacy is present in case of $MnFe_2O_4$ MNPs in addition to the prerequisites of size, crystallinity, magnetization. In case of implementing $Fe(acac)_3$ and $Mn(acac)_2$ (2:1) as precursors and solely ODA in triple role of surfactant, reducing agent and solvent, free NH_2 groups on the surface of $MnFe_2O_4$ MNPs were isolated (aminated=AmMNPs). On the other hand, the decomposition of the same ratio of precursors in the presence of ODA as a surfactant in an aprotic solvent (diphenyl ether) resulted to non-aminated $MnFe_2O_4$ MNPs (Non-AmMNPs). Additionally, the trivalent instead of the divalent manganese acetylacetonate precursor has been used for the synthesis of $MnFe_2O_4$ MNPs as higher magnetization values were expected. The similar decomposition/dissociation rate of Mn^{III} with that one of Fe^{III} precursor can lead to variations of manganese ions in tetrahedral (T_d) and octahedral (O_h) sites in the spinel structure[23] and eventually to higher magnetization values. However, the isolated $MnFe_2O_4$ MNPs with the divalent Mn^{II} precursor showed higher magnetization values (64 emu/g) instead to those of Mn^{III} precursor (10 emu/g) (Figure S1), and under this evidence we did not proceed further with this sample. Further studies are needed to unveil and manipulate the physicochemical properties of MNPs prepared with Mn^{III}. In case of Non-AmMNPs prepared with the divalent precursor the magnetization properties (M_s = 44 emu g^{-1}) allowed us to continue our studies (Figure S7d). TEM images of aminated and non-aminated MNPs are illustrated in Figure 1. Both samples, AmMNPs (Figure 1a) and Non-AmMNPs (Figure 1b), display nearly spherical shape with average sizes at 11 ± 0.6 and 8.4 ± 0.3 nm respectively. The size differences are attributed on the applied synthetic conditions. It has to be noted that the difference in M_s values between the AmMNPs (64 emu/g) and Non-AmMNPs (44 emu/g) is attributed to the size difference. The M_s value decreases as the particle sizes decrease.

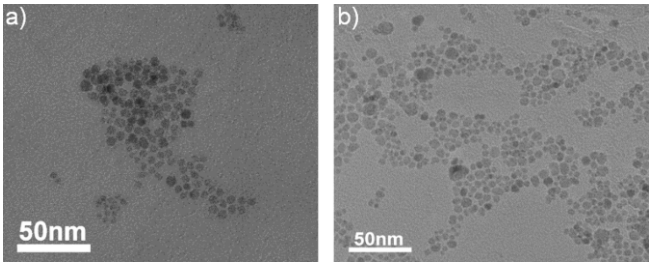

Figure 1. TEM images of AmMNPs (a) and Non-AmMNPs (b).

Aminated $MnFe_2O_4$ MNPs

The powder X-ray diffraction diagram of the sample showed all the characteristic peaks of pure manganese ferrite, while the

average crystalline size of the sample was calculated by fitting the diffraction data with a pseudo-Voigt function (Jade6 Software) and was found 12 nm (Figure S2a). The presence of the organic coating bearing free amines was certified by FT-IR spectroscopy (Figure S2b), while by thermogravimetric analysis (Figure S2c) the total weight loss of the organic coating was measured at 30 % w/w. By taking into account that decomposition occurs in two steps and the linearity of ODA molecules, a configuration of a double layer on the top of the NPs is proposed, with the amines of the inner layer facing the metal ions and those of the outer layer remaining exposed for the formation of the amide bonds with the drugs. The presence of $-NH_2$ group on the MNPs surface was further confirmed by ninhydrin colorimetric assay through the absence or appearance of Ruhemann's purple complex at $\lambda_{max} \approx 600$ nm. The free $-NH_2$ groups were found 0.0035 mg mL^{-1}. The saturation magnetization (M_s) and the coercive field (H_c) value of the MNPs was found 64 emu g^{-1} and 260 Oe, respectively (Figure S2d).[24,25] Detailed characterization of the AmMNPs is given in the SI.

Direct Coupling Functionalization

The direct coupling of NSAIDs was achieved via the formation of a covalent amide bond between the carboxyl groups of the drugs and the NH_2 group of ODA (AmMNPs).[26] FT-IR spectra illustrates the presence of the drug along with the organic coating of the MNPs. Figure 2a clearly shows the absence of the free NH_2 peak at $\approx$ 3300 cm^{-1} presented in the as-prepared MNPs. Moreover, by comparing the spectra of the functionalized MNPs with those of neat NSAIDs (Figure S3), the attenuation of the vibration of carboxylic acid at $\approx$ 1730 cm^{-1} of the NSAIDs is recorded. Simultaneously, FT-IR spectrum of AmMNPs display peak at $\approx$ 1660 cm^{-1} attributed to hydrogen bonding between the surfactant molecules, while in case of MNPs@NSAIDs peaks at $\approx$ 1630 (C=O), $\approx$ 1550–1535 cm^{-1} (N–H) correspond to amide I and at $\approx$ 1450 cm^{-1} amide II (C–N) vibrations. The spectrum of MNPs@ASA demonstrates also peak at $\approx$ 1700 cm^{-1} characteristic of carbonyl ester vibration. UV/Vis spectra followed the ninhydrin colorimetric analysis further confirmed that $-NH_2$ groups take part in the amide bond after the reaction with NSAIDs, since the absence of Ruhemann's purple complex is observed (Figure 2b). By combining the above data, it can be deduced that the drugs were mostly covalently linked with the MNPs. However, the absorption of small quantity of the drugs onto MNPs cannot be excluded.

Estimation of Drug Loading by Defining the Optimum pH

The efficacy of the nanoplatforms is pH-sensitive and thus a comparative study in the pH region 2 to 8 was undertaken in order to define the appropriate pH values for the calculations of drug loading and release. Solubility and permeability are the two important characteristics that define the pharmacokinetic profile of the drugs.[27] The balance between the dissolution rate and the absorption through lipid membranes in combination with the targeted area of application determine the performance of the functionalized MNPs.[28] For example, the pH of gastric acid is 1.5 to 3.5, whereas the pH gradually increases in the small intestine from pH 6 to approximately 7.4 in the terminal ileum. In so, ASA at pH > 5 exists in its ionic form

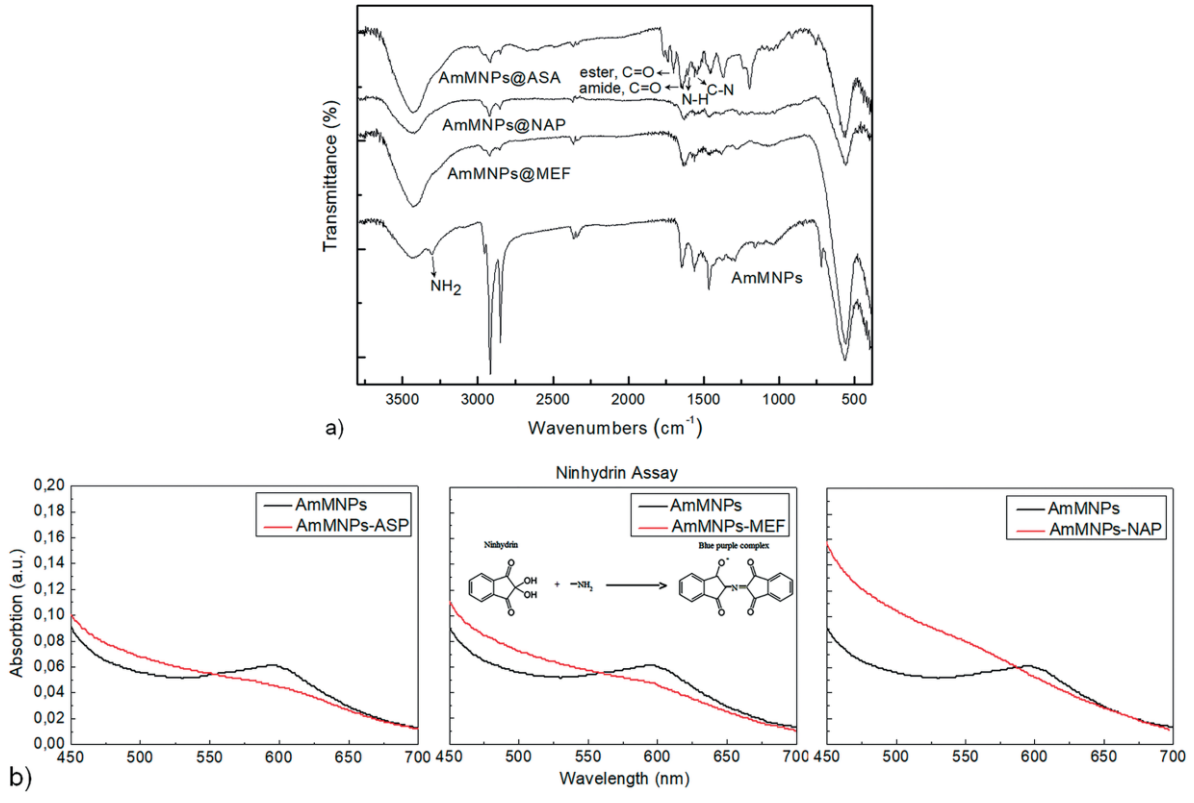

Figure 2. (a) FT-IR spectra of AmMNPs directly coupled with ASA, MEF and NAP in comparison with as prepared MNPs. (b) Ninhydrin colorimetric analyses showing the absence of free NH_2 groups after the formation of amide bond.

(R-COO$^-$) with high aqueous solubility, but lower absorption through lipid membranes, whereas at pH < 2 a neutral form (R-COOH) is formed which lowers the aqueous solubility by simultaneously enhancing the absorption.[28] The mixture of the two forms existing at the pH region of 2–5 seems to be the key of balanced dissolution and absorption rate.[28] As far as mefenamic acid concerned the dissolution rate increases with pH reaching its maximum at pH = 9.[29] In case of NAP, the solubility is low at the pH region 2.2 to 5.8 due to unionization of drug, while an intermediate dissolution rate is recorded at pH = 6.4. At pH = 7.4 the solubility of the drug further improves, but the permeability gets extremely low.[27] In order to define the optimum pH for each drug, the stability of ODA in variable pH was also investigated. Based on previous report, ODA molecules are almost neutral charged at pH > 5.7 and thus the layer is stable, while in the pH 3–4 the amine headgroups get protonated and the ODA molecules either dissolve into the solution subphase or are positioned loosely at the interface. By lowering the pH further (< 3), ODA molecules form a layer but with defects.[30] UV measurements were conducted in order to estimate the drug loading in different pH based on the respective reference curves (Figures S4–S6). After all, by combining all the remarks, the optimum pH values for ASA, MEF and NAP studies were set as 2.2, 7.4 and 6.4, while the loaded drug was estimated ≈ 13.5 % w/w, 39.7 % and 27 % w/w, respectively.

The hydrodynamic sizes in terms of Z-average (d.nm) with the relative polydispersity indexes (pdI) of the functionalized by direct coupling MNPs, AmMNPs@ASA, AmMNPs@MEF and AmMNPs@NAP, were measured in PBS and found 166.3 nm (0.341), 220 nm (0.277) and 247.4 nm (0.205), respectively. The primary AmMNPs were found with diameter of 137.8 nm (0.160), implying that the functionalization process did not alter significantly the physicochemical properties of the MNPs. The pH-dependent zeta potential was measured for the functionalized MNPs and is shown in Figure 3. Zeta potential measurements allow us to follow the charge of the nanoparticles in different environments and to determine the point of zero charge (PZC) which is the pH at which there is no charge on the nanoparticles' surface.[31,32] AmMNPs@ASA and AmMNPs@NAP displayed positive zeta potential (> +15 mV) at low pH (< 3), with PZC occurring at pH ≈ 6 and 5, respectively. Though at the pH range 3.5–7 the values were varied from +13 to –4 mV, the particles were stable and no precipitation was observed,

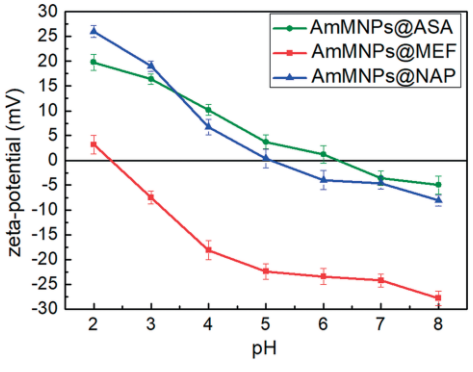

Figure 3. Zeta potential as a function of pH for AmMNPs@ASA, AmMNPs@MEF and AmMNPs@NAP.

indicating that steric stabilization contributes to the colloidal stability. In case of AmMNPs@MEF the PZC was recorded at pH ≈ 2.5, while at pH > 4 negative zeta potential values were recorded (from –18 to –22 mV). In all cases, hydrodynamic sizes indicate that aggregation took place probably via Van der Waals interactions, while the zeta potential values were less than ±30 mV, which is generally considered as the threshold value for electrostatic stabilization.[33]

Non-Aminated $MnFe_2O_4$ MNPs and PEGylation of the MNPs

The powder X-ray diffraction diagram of the sample showed all the characteristic peaks of pure manganese ferrite, while the average crystalline size of the sample was calculated by fitting the diffraction data with a pseudo-Voigt function (Jade6 Software) and was found 9 nm very close to the size provided by TEM (Figure S7a). The encapsulation of Non-AmMNPs into PEG matrix was initially carried out without any drug. In the FT-IR spectra (Figure S7b) the peaks of Non-AmMNPs, clearly shown at ≈ 489 and 600 cm^{-1}, are corresponding to the manganese and ferrite oxides, respectively. By comparing the spectra of Am-MNPs and Non-AmMNPs, the disappearance of the NH_2 group peak at ≈ 3300 cm^{-1} is recorded only in the last case, indicating the absence of free amines onto the MNPs. Thermogravimetric analysis data of Non-AmMNPs demonstrate that ODA, despite the fact that is absorbed at higher percentage (weight loss 50 %), is getting decomposed at one step (Figure S7c), whereas in case of Am-MNPs two layers of the surfactant were observed. Although AmMNPs were found of enhanced M_s value, still Non-AmMNPs display appropriate magnetic properties (Figure S7d). The detailed characterization is given in the SI.

Loading on the PEG Matrix

Encapsulation of NSAIDs in colloidal nanodispersions represents a promising strategy with the significant potential for enhancement of bioavailability. PEGylation is a commonly used procedure for providing "stealth" characteristics, since enable the MNPs to deceit RES.[34] The amphiphilic properties of PEG polymers (molecular mass lower than 100 kDa) allow for entrapment of the MNPs through a biphasic system ($H_2O/CHCl_3$) without the need of any other linker. Under that prism, PEG8000 created a polymeric matrix around the MNPs where the drugs were loaded/adsorbed in a second step through Van der Waals interactions and hydrogen bonding. Drug loading on PEGylated Non-AmMNPs was utilized as an alternative functionalization method. PEG8000 was used for the loading of ASA, MEF and NAP on the MNPs in order to study the release rate compared to the AmMNPs directly coupled with the drugs. Although there is a permanent interest to enhance the aqueous solubility and dissolution rate of NSAIDs in order to achieve faster onset of action and to minimize the absorption variability, the simultaneous encapsulation of MNPs and NSAIDs is scarcely reported.[35]

The presence of the drugs onto the PEG chains of the Non-AmMNPs was evidenced by FT-IR spectroscopy. The characteristic vibrations of methylene groups of PEG chains at ≈ 2934 cm^{-1}, multiple CH_2–O–CH_2 vibration modes at ≈ 1107 cm^{-1}, and carboxylic group at ≈ 1640–1700 cm^{-1} of

the drugs, respectively, are presented in Figure 4. The peaks corresponding to ODA have been shaded by those of the bulkier PEG8000, while in case of ASA, MEF and NAP the bending vibration of –C–H group is depicted at ≈ 1380 cm^{-1}. Moreover, in case of MEF the peak at ≈ 700 cm^{-1} corresponds well with bending vibration of –NH. The relative amounts of ASA and NAP were estimated ≈ 18.8 % and 24.2 % w/w at pH 2.2 and 6.4 respectively, of the total mass of the samples by UV measurements (Figure S4, Figure S6). However, in case of MEF, countable amount of ODA molecules was released together with the drug at pH 7.4, implying a loose conformation of the surfactant layer on the surface of the MNPs and in that case quantification was not allowed.

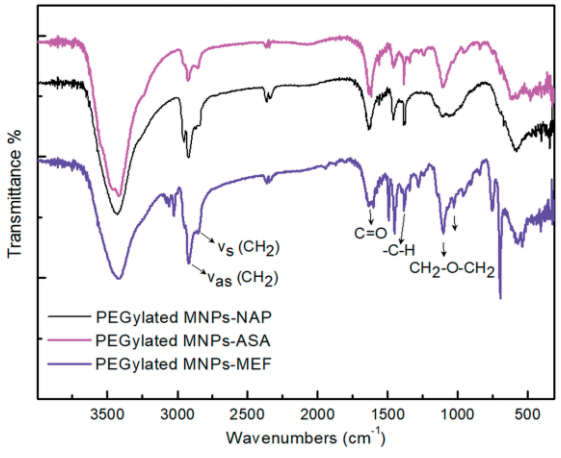

Figure 4. FT-IR spectra of PEGylated Non-AmMNPs loaded with ASA, MEF and NAP.

The hydrodynamic sizes of the PEGylated Non-AmMNPs loaded with the drugs were measured in PBS. The relative diameters were found 178.7 nm (pdI:0.277) and 194.6 (pdI:0.189) for Non-AmMNPs@PEG-NAP and Non-AmMNPs@PEG-ASA, respectively, indicating that those systems slightly differ from the analogous direct functionalized MNPs. This is attributed to the relatively low molecular weight of PEG and/or to the low amount of the polymer. The zeta potential values varied from +20 to +25 mV, while the dispersions were stable in the pH range 2–9 and no precipitation occurred. In case of PEGylation, steric stabilization dominates making electrostatic repulsions insignificant.[36]

Drug Release

The drug release studies of the functionalized samples were conducted in diverse pH according to the stability and dispersion of the drugs in conjugation with minimization of the dissolution of ODA molecules. The release profile corresponds well with a two-step procedure. The Ritger–Peppas model was applied to estimate the drug release rate in each case. The estimation of cumulative release in percentage (Q) after 3 h and 24 h is presented in Table 1. In case of direct coupling functionalization, the covalent attachment of the drugs onto MNPs resulted in lower Q_{24h}% drug release, since the amide bond is more stable.[37] The cumulative NAP and ASA release in percentage (Q) after 24 h was estimated 34.6 %, and 42 %, respectively, while in case of MEF the respective percentage hardly reaches 20.8 %. On the other hand, the percentages of drug release from the PEG matrix were significantly higher up to 24 h (91 % NAP and 62 % ASA release), due to the weaker Van der Waals interactions between the adsorbed NSAIDs and the PEG chains.

Table 1. Percentage of cumulative release (Q%) at 3 h and 24 h and release exponent (*n*) according to Ritger–Peppas model.

	n_{3h}	Q_{3h}%	n_{24h}	Q_{24h}%
AmMNPs@ASA	0.63	32	0.2	42
AmMNPs@MEF	0.66	17	0.09	20.8
AmMNPs@NAP	0.45	27	0.1	34.6
Non-AmMNPs@PEG-NAP	> 1	66	0.14	91
Non-AmMNPs@PEG-ASA	0.28	38	0.18	62

In all cases of amide bond formation, under the assumption that there is not observed any swelling phenomena and the nanoparticles remain spherical, the respective limits of the diffusion index *n* were implemented to determine the mechanistic aspects of the drug release. The estimated n_{3h} value indicated a non-Fickian diffusion ($0.43 < n < 1$) and suggested that the release profile is a combination of both diffusion and erosion by means of the amide bond hydrolysis.[38] The second step shows a very small diffusion exponent that can be ascribed to a long-term release (sustained) process mainly due to the stability of the amide bond between ODA and the NSAIDs located in the inner organic layer (Figure 5a).[39] In the case of PEGylated MNPs the limits of the diffusion index *n* differ, since the polymer swelling phenomenon is observed. In case of ASA the diffusion index *n* remains low through time, which is indicative of limited swelling and Fickian diffusion in one stage opposite to NAP, where two stages were recorded. In the latter case the diffusion exponent had a high value ($n_{3h} > 1$) for the first 5 h that indicates a case II transport mechanism. The non-Fickian diffusion is associated with stresses and state-transition of the hydrophilic PEG8000 chains that swell in physiological solution. The lower value ($n_{24h} = 0.14$) for the rest 19 h corresponds to Fickian diffusion and a sustained release from the intermediate layers of the polymer is indicated. We assume that the chemical structure and the smaller size of the acetylsalicylic acid as well as the stronger Van der Waals interactions and hydrogen bonding between the molecule and the polymer could justify the above remark (Figure 5b).

By comparing the release profile of NAP among the two ways of functionalization, direct coupling and PEGylation, different release profiles are revealed. In the first case, the hydrolysis of the amide bond of the outer layer is followed by hydrolysis occurring in the inner coating. On the other hand, when NAP is loaded on PEG matrix, the release is happening via diffusion from the outer polymer layer due to polymer swelling, while later NAP molecules that are more protected are released by interlayer diffusion among the stacking of PEG chains. Similar behavior was recorded when ASA and MEF molecules were directly coupled onto the aminated MNPs. However, when ASA is adsorbed on PEG matrix, the diffusion remains gradual but the release records higher cumulative percentages.

It is worth to mention that direct coupling proved to be a simple and efficient method for incorporating ASA, MEF and NAP and achieve a sustained therapeutic release rate. Moreover,

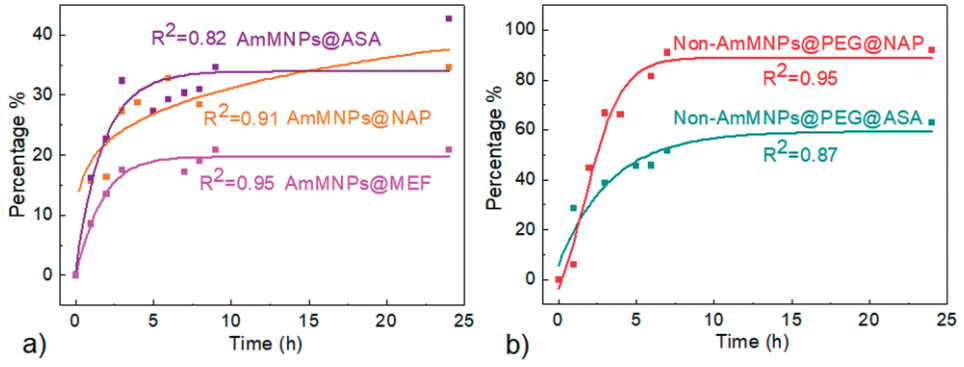

Figure 5. (a) Comparative cumulative drug release in percentage (Q %) for direct functionalization in a 24 h time period, (b) Comparative cumulative drug release in percentage (Q %) for PEGylated MNPs-NSAIDs in a 24 h time period. Adjusted R-squared values are also included.

it does not require preliminary modifications that would cause the loss of NSAIDs activity and any external source to trigger the drug release.[40]

2.2. Anti-Inflammatory Activity of MNPs and Functionalized MNPs

Evaluation of Lipoxygenase Activity

NSAIDs are primarily COX inhibitors and exert their activity by reducing the production of PGs induced in the inflammatory process. In recent years, it has been clarified that PG synthesis is only one part of the arachidonic acid pathway.[41] Eicosanoids are oxygenated metabolites of arachidonic acid and they are implicated in a diversity of diseases. Lipoxygenase (LOX) catalyzes the first two steps in the metabolism of arachidonic acid to leukotrienes (LTs) which are important in the pathogenesis of neutrophil-mediated inflammatory diseases.[42] In view of this concept dual inhibition of the COX and LOX pathways could produce a wider spectrum of anti-inflammatory effects and thus the ability of nanoplatforms to inhibit soybean lipoxygenase (LOX) was tested.

The results presented in Table 2 demonstrate that solely the MNPs (either aminated or not) did not interfere with the ability of LOX to bind with its substrate, in the tested concentrations. However, the functionalized MNPs inhibited the LOX activity with IC_{50} values comparable with the neat drugs (controls), while the anti-inflammatory activity of the nanoplatforms does not seem to be affected by the way of functionalization. MNPs coupled/loaded with ASA recorded the most remarkable function (respective IC_{50} values; 6.7, 7.6 μg/mL) and for this reason was selected to be studied further.

Table 2. Anti-inflammatory activity of AmMNPs and Non-AmMNPs before and after functionalization with NSAIDs evaluated by the half-minimal inhibitory concentration (IC_{50}) (μg/mL). Data represented are mean ±SD of three identical experiments made in three replicates.

	LOX Inhibition IC_{50} (μg/mL)
AmMNPs	> 50
Non-AmMNPs	> 50
AmMNPs@ASA	6.7 ± 0.89
AmMNPs@MEF	12 ± 0.94
AmMNPs@NAP	8.4 ± 0.76
Non-AmMNPs@PEG-ASA	7.6 ± 0.92
Non-AmMNPs@PEG-NAP	9.8 ± 0.78
ASA	5.2 ± 0.45
NAP	5.5 ± 0.87

Albumin Denaturation Experiments

Protein denaturation is a process during which the secondary and tertiary structures of proteins are destroyed resulting in loss of their biological function caused by a spectrum of reasons including heat, electrolytes, or alcohols which generate well-studied alterations in the solubility of albumins and globulins.[43] Inflammation and protein denaturation are closely related, and inhibition of the protein collapse is achieved by NSAIDs. Acetylsalicylic acid has shown a dose-dependent ability to inhibit the induced protein denaturation.[44] Zinc peroxide, silver and iron nanoparticles have also been tested as anti-inflammatory agents via inhibition of denaturation and have been found of concentration dependent anti-inflammatory activity.[45,46,47] Herein, we aimed at examining both the anti-inflammatory capacity of $MnFe_2O_4$ MNPs and the collective properties of MNPs coupled and/or loaded with ASA. Protein denaturation was triggered by heating and acidifying of bovine serum albumin (BSA), which results in antigen expression and is related with type-III hypersensitivity reaction, which in turn is associated to various diseases including rheumatoid arthritis, systemic lupus erythematosus, serum sickness, and glomerulonephritis.[48] The assay implemented is based on albumin denaturation optical density measurements and results derived from 5 different concentrations (5, 10, 25, 50, and 100 μg/mL). Results are summarized in Table 3 where ASA values are also included as reference.

Denaturation of albumin in the presence of PBS is considered as 0 % anti-inflammatory activity, while in all cases the observed action is concentration dependent. AmMNPs and Non-AmMNPs protected the protein unfolding but in lower extent compared to the reference drug. However, in case of functionalized MNPs (AmMNPs@ASA and Non-AmMNPs@PEG-ASA) a much stronger anti-inflammatory capacity comparable with that of free ASA is recorded. The higher % protective ability against protein denaturation is recorded when ASA is directly coupled with the MNPs (82.5 %), which implies enhanced anti-inflammatory response. Still, Non-AmMNPs@PEG-ASA display a high protection value (79.7 %) towards albumin denaturation.

Table 3. Anti-inflammatory activity of various concentrations [0 (control), 5, 10, 25, 50, and 100 μg/mL] of AmMNPs and Non-AmMNPs before and after functionalization with ASA, as well as ASA (reference drug), measured as inhibitory percentage (%) of albumin denaturation. Data represented are mean ±SD of three identical experiments made in three replicates.

Concentration (μg/mL)	Denaturation protection/Anti-inflammatory activity [%] AmMNPs	Non-AmMNPs	AmMNPs@ASA	Non-AmMNPs@PEG-ASA	ASA
0 (control)	0	0	0	0	0
5	7.9 ± 0.84	6.7 ± 0.79	12.4 ± 0.76	10.9 ± 0.65	11.2 ± 0.77
10	10.9 ± 0.88	9.2 ± 0.97	21.5 ± 0.75	16.1 ± 0.65	25.3 ± 0.54
25	23.7 ± 0.99	19.6 ± 0.66	48.8 ± 0.53	43.6 ± 0.69	47.6 ± 0.78
50	34.9 ± 0.49	30.6 ± 0.78	63.2 ± 0.74	51.4 ± 0.94	65.7 ± 0.43
100	57.2 ± 0.64	48.4 ± 0.39	82.5 ± 0.59	79.7 ± 0.86	88.9 ± 0.58

3. Conclusions

Diagnostic and therapeutic agents in complicated diseases, which are correlated with chronic inflammation (e.g. cancer, Alzheimer's Disease), are one of the most promising aspects of nanotechnology to be implemented in human health. The design and drug loading of nanoplatforms is challenging, as unique release profiles can be exploited in different diseases. The physicochemical properties of the magnetic nanocarriers as well as those of drugs, have to be combined properly for the desired outcome. ODA as a primary surfactant proved to be a beneficial agent for synthesizing $MnFe_2O_4$ MNPs of high crystallinity, with superparamagnetic behavior and based on the synthetic conditions with aminated or non-aminated surface, which further can be tuned either by direct or indirect functionalization processes, respectively. Three different NSAIDs (carboxylate donors) were successfully coupled with the aminated MNPs via formation of amide bond, as well as encapsulated with Non-AmMNPs in a PEG matrix. In case of the covalent attachment of ASA, MEF and NAP with the MNPs sustained drug release was observed, whereas more rapid release profiles were recorded when NSAIDs loaded onto PEGylated MNPs. The balance between the dissolution rate of the drugs and the absorption through lipid membranes is affected by the pH of the targeted area and eventually the drug loading and release was found pH-sensitive. The in vitro studies indicate that functionalized MNPs could be administered to a variety of inflammatory conditions, depending on the release profile, giving the perspective to propose these nanocarriers as theranostics.

4. Experimental Section

Materials: All the reagents were used without any further purification. Iron(III) acetylacetonate [$Fe(acac)_3$] and octadecylamine (> 90.0 %) were purchased by Fluka, while manganese(II) acetylacetonate [$Mn(acac)_2$, ≥ 99.9 %] was supplied by Sigma-Aldrich. Ethanol (100 %, 1 % MEK) was from Bruggermann GmbH and chloroform (analytical reagent) from Chem. Lab NV. Diphenyl ether (DPE) and ninhydrin (GR for analysis ACS, Reag. Ph Eur) were purchased by Merck. Phosphate buffer pH 6.4 and 7.4 was prepared with NaH_2PO_4 (Merck), Na_2HPO_4 (Merck) and NaCl (Merck), while phosphate buffered saline (PBS, pH = 7.2) was obtained by E.U Gibco BRL. 1-(3-Dimethylaminopropyl)-3-ethylcarbodiimide hydrochloride, (EDC, > 98.0 %, coupling agent for peptides) was purchased from TCI (Tokyo Chemical Industry) and PEG8000 from Alfa Aesar GmbH & CoKG. Triethylamine (Et_3N, ≥ 99.5 %), *N*-hydroxysuccinimide (NHS, 98.0 %) and acetylsalicylic acid (ASA) were from Sigma-Aldrich. (*S*)-(+)-2-(6-methoxy-2-naphthyl)propionic acid (Naproxen) and Mefenamic acid (MEF) was from Aldrich Chemistry. Deionized water was used for the fabrication of $MnFe_2O_4$ MNPs and Milli pure water (< 3.0 MR, Millipore, MilliQ Gradient) was used for the modification of the NPs surface properties. Nanofilters Minisart RC 15 (Single use syringe filter Non-sterile RC-membrane, Pore Size: 0.20 μm) were from Sartorius Stedim Biotech GmbH. Pur-A-Lyzer Midi 1000 Dialysis Kit (for Research & Development use only) by Sigma-Aldrich. Bovine serum albumin was purchased from Sigma (1 % aqueous solution, Sigma-Aldrich, Germany).

Characterization Techniques: Powder X-ray diffraction (XRD) was performed using a 2-cycle Rigaku Ultima+ diffractometer (40 kV, 30 mA, Cu-K_α radiation) with Bragg–Brentano geometry (detection limit 2 % approximately). Fourier transform infrared spectroscopy (280–4000 cm^{-1}) was recorded using a Nicolet FTIR 6700 spectrometer with samples prepared as KBr pellets. Thermogravimetric analysis (TGA) was performed using a SETA-RAM SetSys-1200 instrument at a heating rate of 10 °C min^{-1} under N_2 atmosphere. Magnetic measurements were acquired by a vibrating sample magnetometer (1.2H/CF/HT Oxford Instruments VSM). The isolation of the organic coating was achieved after the dissolution of the samples in $CHCl_3$ and several cycles of sonication and centrifugation, until the supernatant was limpid. The supernatant from each washing cycle was removed and placed into glass vials. Then it was filtered with the use of nanofilters to retain the dispersed NPs. UV/Visible measurements were carried out with a double beam UV/Visible spectrophotometer U-2001 Hitachi. The dynamic light scattering (DLS) and zeta potential measurements were performed with a Malvern Zetasizer instrument. Conventional TEM images were obtained with a JEOL 100 CX microscope (TEM), operating at an acceleration voltage of 100 kV. For TEM observations we have used suspensions of the nanoparticles deposited onto carbon-coated copper TEM grids.

Preparation of $MnFe_2O_4$ MNPs with Amine Groups on the Surface (AmMNPs): $MnFe_2O_4$ MNPs with aminated surface (AmMNPs) were prepared in an autoclave by the decomposition of acetylacetonate iron(III) and manganese(II) at a 2:1 ratio, $Fe(acac)_3$ 1.8 mmol/$Mn(acac)_2$ 0.9 mmol in the presence solely of ODA 12.9 mmol. The temperature of the oven was elevated with a steady rate (4 °C/min) to 200 °C and was kept stable for 24 h. After the 24 h reaction the autoclaves were left to cool down to room temperature with a rate of 5 °C/min and $MnFe_2O_4$ MNPs were isolated after repeated washing cycles with EtOH and centrifugation (5000 rpm).

Direct Coupling of Acetylsalicylic Acid, Mefenamic Acid, and Naproxen on AmMNPs: The direct coupling of NAP onto the AmMNPs surface coating was achieved via a modified procedure,[49] where 20 mg of AmMNPs were mixed with EDC (47.9 mg), NHS (≈ 3 mg), ASA (45 mg), MEF (60 mg), NAP (57.5 mg) and Et_3N (0.1 mL) in $CHCl_3$ (5 mL). The mixture was shaken vigorously for

24 h and the AmMNPs-NSAIDs were isolated after repeated washing cycles with EtOH and centrifugation.

Preparation of Non-Aminated $MnFe_2O_4$ MNPs (Non-AmMNPs): Non-aminated $MnFe_2O_4$ MNPs were prepared in an autoclave by the decomposition of acetylacetonate iron(III) and manganese(II) as described in case of AmMNPs, while in the amount of ODA (0.998 mmol) and DPE (7 mL) was constant. The temperature of the oven was elevated with a steady rate (4 °C/min) to 200 °C and remained stable for 24 h. After the 24 h reaction the autoclaves were left to cool down to room temperature with a rate of 5 °C/min and $MnFe_2O_4$ MNPs were isolated after repeated washing cycles with EtOH and centrifugation (5000 rpm).

Loading of Acetylsalicylic Acid, Mefenamic Acid, and Naproxen on Non-AmMNPs: A 3 mL of solution of Non-AmMNPs in $CHCl_3$ (5 mg mL^{-1}) was added dropwise in a 25 mL of solution of PEG8000 in H_2O (3.2 mg mL^{-1}), the two-phase mixture was sonicated in a cold sonication bath (25–30 °C) for ≈ 2 h until a stable emulsion was formed (high temperature prevents the formation of a stable emulsion). After ≈ 2 h, 40 mg of PEG8000 were added in the emulsion and sonication was applied for 30 min. The $CHCl_3$ was evaporated from the system with elevation of temperature of the sonication bath and then the solution was left to cool to room temperature. 120 mg of PEG8000 were added in the solution a new followed by the addition of 2 mL of NSAIDs (8 mg of ASA, 10.5 mg of MEF, 10 mg of NAP) in $CHCl_3$ (5 mg mL^{-1}). The emulsion was sonicated again for 2 h and $CHCl_3$ was evaporated. The Non-AmMNPs@PEG-NSAIDs was isolated through washing and centrifugation cycles with EtOH and was dried under vacuum.

Drug Release: For the drug release study, ≈ 3 mg of the functionalized MNPs were placed into a Pur-A-Lyzer Midi 1000 dialysis membrane. The membrane floated in 45 mL of phosphate buffer solution (PBS pH 6.4 and 7.4) or buffer HCl/NaCl (pH 2.2) and was shaken (200 rpm) at 35 °C. In certain time intervals 2 mL of the medium were removed and replaced with fresh PBS solution. This procedure was followed for both AmMNPs-NSAIDs and Non-AmMNPs@PEG-NSAIDs, as well as for ASA, MEF and NAP. UV measurements were recorded at 265 nm and the cumulative release in percentage (Q%) was calculated and plotted against time according to Equation (1)[16]:

$$Q_n\,\% = \left(\frac{\left(\left(\left(\frac{A_n \times V}{A_s} \right) + \left(\frac{((A_{n-1} + A_{n-2} + \cdots) \times R)}{A_s} \right) \right) \times C \right)}{W} \right) \times 100 \quad (1)$$

where, A_1 is the absorption of the first medium removal, A_2 the absorption of the second medium removal, A_n is the absorption of the n_{th} medium removal, A_s (absorption of the standard) for each sample, V is the total volume of the medium (mL), C concentration of the standard (mg mL^{-1}), W weight of the active compound [mg (label claim)], R removed medium volume (mL) and n is the removal number. The release profiles were estimated by using Ritger–Peppas equation [Equation (2)][50–52]

$$Q = kt^n \quad (2)$$

where Q is the cumulative drug release in percentage, t is the release time in hours, k is a rate constant reflecting the structural and geometric characteristics of the carriers, and n is the release component that corresponds to the release mechanism of the drug.

Ninhydrin Colorimetric Assay: Aliquots of 0.1–0.6 mL of ODA (0.25 mg mL^{-1}) in DMF were pipetted into a series of tubes.[53] 0.7 mL of ninhydrin solution in MeOH 0.06 M (10.7 mg mL^{-1}) were added in each tube, mixed well and heated in a water bath at 100 °C for 5 min. After a short heating period (5 min) the color of the solution changed (formation of Ruhemann's purple) and the content was transferred to a 5 mL volumetric flask and was diluted with DMF for the UV/Vis absorbance measurement. A suspension of MNPs in DMF (0.25 mg mL^{-1}, stock) was prepared accordingly for all the samples (AmMNPs, Non-AmMNPs before and after functionalization) and 0.4 mL of each stock solution was pipetted into boiling tubes with 0.7 mL of ninhydrin solution following the same procedure described above. The absorbance of the formed complex (Ruhemann's purple) was recorded at ≈ 600 nm.

Evaluation of Anti-Inflammatory Activity

1. Evaluation of Lipoxygenase Activity: The reaction mixture contained (final concentration) the MNPs (AmMNPs, Non-AmMNPs before and after functionalization with NSAIDs), dissolved in water at concentrations of 2–50 μg/mL, or the solvent (control), soybean lipoxygenase, dissolved in 0.9 % NaCl solution (250 mg mL^{-1} final concentration) and sodium linoleate (100 μM), in Tris/HCl buffer, pH 9.0. The reaction was monitored for 9 min at 28 °C, by recording the absorbance of a conjugated diene structure at 234 nm, due to the formation of 13-hydroperoxy-linoleic acid. The performance of the assay was checked using aspirin and naproxen as reference drugs.

2. Albumin Denaturation Experiments: To evaluate the anti-inflammatory activity of MNPs and functionalized MNPs with ASA, a modified assay studying bovine serum albumin denaturation was implemented.[54] In detail, MNPs were mixed with 1 % w/v PBS solution of bovine albumin to reach final concentration of 5, 10, 25, 50 and 100 μg/mL. The mixtures were incubated at 37 °C for 20 min, and subsequently 200 μL of HCl 6 M were added to each sample, while the temperature was raised at 51 °C and kept for 2 min to prop up the denaturation of albumin. The turbidity of the solutions was measured spectrophotometrically at 660 nm. ASA was used as the reference drug. Denaturation of albumin in the presence of distilled water is considered as 100 % denaturation. The protection of protein denaturation (%), hence the anti-inflammatory activity of MNPs was calculated according to Equation (3):

$$\%\ \text{Protection} = 100 - \left(\frac{OD\ of\ sample\ \ tested}{OD\ of\ control} \right) \text{x}\ 100 \quad (3)$$

Where OD refers to the turbidity values at OD_{660} nm and control refers to the aqueous solution of 1 % bovine albumin in distilled water.

Acknowledgments

The authors would like to thank Dr. D. Sakellari for her assistance in TEM imaging.

Keywords: Manganese · Magnetic properties · Nanoparticles · Biological activity · Functionalized nanoplatforms · Drug delivery

[1] C. Carbone, T. Musumeci, R. Pignatello, *Woodhead Publ., Ser. Biomed.* **2013**, 281–303.
[2] L. Gasparini, E. Ongini, G. Wenk, *J. Neurochem.* **2004**, *91*, 521–536.
[3] M. S. Saito, *J. Hematol. Transfus.* **2016**, *4*, 1040.

[4] M. M. Wen, R. M. Farid, A. A. Kassem, *J. Liposome Res.* **2014**, 1532–2394.
[5] K. C. Patel, S. Pramanik, *World J. Pharm. Pharm. Sci.* **2014**, *3*, 1391–1405.
[6] P. Yammine, D. Moussa, M. Ayrouth, R. Kassab, *IJPSR* **2017**, *8*, 3347–3353.
[7] S. Patnaik, A. Dileep Kurdekar, L. Adinarayana Avinash Chunduri, C. Prathibha, K. Venkataramaniah, *JDDMC* **2017**, *3*, 77–85.
[8] O. C. Farokhzad, R. Langer, *ACS Nano* **2009**, *3*, 16–20.
[9] P. Couvreur, *Adv. Drug Delivery Rev.* **2013**, *65*, 21–23.
[10] E. Blanco, H. Shen, M. Ferrari, *Nat. Biotechnol.* **2015**, *33*, 941–951.
[11] D. Rosenblum, N. Joshi, W. Tao, J. M. Karp, D. Peer, *Nat. Commun.* **2018**, *9*, 1410.
[12] O. Veiseh, J. W. Gunn, M. Zhang, *Adv. Drug Delivery Rev.* **2010**, *62*, 284–304.
[13] K. McNamara, S. A. M. Tofail, *Phys. Chem. Chem. Phys.* **2015**, *17*, 27981.
[14] K. Ulbrich, K. Holá, V. Šubr, A. Bakandritsos, J. Tuček, R. Zbořil, *Chem. Rev.* **2016**, *116*, 5338–5431.
[15] I. M. El-Sherbiny, N. M. Elbaz, M. Sedki, A. Elgammal, M. H. Yacoub, *Nanomedicine (Lond.)* **2017**, *12*, 387–402.
[16] V. Georgiadou, G. Makris, D. Papagiannopoulou, G. Vourlias, C. Dendrinou-Samara, *ACS Appl. Mater. Interfaces* **2016**, *8*, 9345–9360.
[17] G. Wang, D. Zhao, Y. Ma, Z. Zhang, H. Che, J. Mu, X. Zhang, Z. Zhang, *Appl. Surf. Sci.* **2018**, *428*, 258–263.
[18] R. Liang, R. Tian, Z. Liu, D. Yan, M. Wei, *Chem. Asian J.* **2014**, *9*, 1161–1167.
[19] V. Biju, *Chem. Soc. Rev.* **2014**, *43*, 744.
[20] T. Miao, J. Wang, Y. Zeng, G. Liu, X. Chen, *Adv. Sci.* **2018**, *5*, 1700513.
[21] L. Kumar, S. Verma, M. Singh, T. Utreja, P. Utreja, *Curr. Drug Delivery* **2018**, 15.
[22] V. Georgiadou, C. Dendrinou-Samara, *Eur. J. Inorg. Chem.* **2014**, 3645–3656.
[23] V. Georgiadou, V. Tangoulis, I. Arvanitidis, O. Kalogirou, C. Dendrinou-Samara, *J. Phys. Chem. C* **2015**, *119*, 8336–8348.
[24] K. Vamvakidis, D. Sakellari, M. Angelakeris, C. Dendrinou-Samara, *J. Nanopart. Res.* **2013**, *15*, 1743.
[25] K. Vamvakidis, M. Katsikini, D. Sakellari, E. C. Paloura, O. Kalogirou, C. Dendrinou-Samara, *Dalton Trans.* **2014**, *43*, 12754–12765.
[26] W. A. Zordok, S. A. Sadeek, W. H. El-Shwiniy, *J. Coord. Chem.* **2012**, *65*, 353–369.
[27] L. Kumar, B. S. Suhas, G. Pai K, R. Verma, *Res. J. Pharm. Technol.* **2015**, *8*, 825–828.
[28] M. Voelker, M. Hammer, *Inflammopharmacology* **2012**, *20*, 225–231.
[29] W. Nurhikmah, Y. C. Sumirtapura, J. S. Pamudji, *Sci. Pharm.* **2016**, *84*, 181–190.
[30] Z. Avazbaeva, W. Sung, J. Lee, M. D. Phan, K. Shin, D. Vaknin, D. Kim, *Langmuir* **2015**, *31*, 13753–13758.
[31] A. Sharma, C. Cornejo, J. Mihalic, A. Geyh, D. E. Bordelon, P. Corangath, F. Westphal, C. Gruettner, R. Ivkov, *Sci. Rep.* **2018**, *8*, 4916.
[32] V. Ayala, A. P. Herrera, M. Latorre-Esteves, M. Torres-Lugo, C. Rinaldi, *J. Nanopart. Res.* **2013**, *15*, 1874.
[33] D. Cunningham, R. E. Littleford, W. E. Smith, P. J. Lundahl, I. Khan, D. W. McComb, D. Graham, N. Laforest, *Faraday Discuss.* **2006**, *132*, 135–145.
[34] K. Giannousi, E. Hatzivassiliou, S. Mourdikoudis, G. Vourlias, A. Pantazaki, C. Dendrinou-Samara, *J. Inorg. Biochem.* **2016**, *164*, 82–90.
[35] S. Agrawal, T. K. Giri, D. K. Tripathi, A. A. Ajazuddin, *Am. J. Drug Discovery Dev.* **2012**, *2*, 143–183.
[36] R. De Palma, S. Peters, M. J. Van Bael, H. Van der Rul, K. Bonroy, W. Laurein, J. Mullens, G. Borghs, G. Maes, *Chem. Mater.* **2007**, *19*, 1821–1831.
[37] S. Patra, E. Roy, P. Karfa, S. Kumar, R. Madhuri, P. Kumar Sharma, *ACS Appl. Mater. Interfaces* **2015**, *7*, 9235–9246.
[38] G. Singhvi, M. Singh, *IJPSR* **2011**, *2*, 77–84.
[39] H. Zhang, D. Pan, K. Zou, J. He, X. Duan, *J. Mater. Chem.* **2009**, *19*, 3069–3077.
[40] K. Werengowska-Ciećwierz, M. Wiśniewski, A. P. Terzyk, S. Furmaniak, *Adv. Condens. Matter Phys.* **2015**, 198175, (pp. 27).
[41] J. Martel-Pelletier, D. Lajeunesse, P. Reboul, J. Pelletier, *Ann. Rheum. Dis.* **2003**, *62*, 501–509.
[42] Z. Boulsourani, G. D. Geromichalos, S. Katsamakas, V. Psycharis, C. P. Raptopoulou, D. Hadjipavlou-Litina, D. Sahpazidou, C. Dendrinou-Samara, *Mater. Sci. Eng. C* **2019**, *94*, 493–508.
[43] H. Neurath, J. P. Greenstein, F. W. Putnam, J. O. Erickson, *Chem. Rev.* **1944**, *34*, 157–265.
[44] T. Morris, M. Stables, A. Hobbs, P. de Souza, P. Colville-Nash, T. Warner, J. Newson, G. Bellingan, D. W. Gilroy, *J. Immunol.* **2009**, *183*, 2089–2096.
[45] S. S. Ali, R. Morsy, N. A. El-Zawawy, M. F. Fareed, M. Y. Bedaiwy, *Int. J. Nanomed.* **2017**, *12*, 6059–6073.
[46] I. Gnanasundaram, K. Balakrishnan, *J. Nanosci. Nanotechnol.* **2017**, *3*, 266–269.
[47] H. Abdulalsalam, N. M. Ardalan, S. H. Ahmed, *Curr. Res. Microbiol. Biotechnol.* **2017**, *5*, 1151–1156.
[48] G. Kishore, G. Siva, E. S. Sindhu, *Int. J. Pharm. Ind. Res.* **2012**, *1*, 211–213.
[49] D. Bartczak, A. G. Kanaras, *Langmuir* **2011**, *27*, 10119–10123.
[50] P. L. Ritger, N. A. Peppas, *J. Controlled Release* **1987**, *5*, 23–36.
[51] P. L. Ritger, N. A. Peppas, *J. Controlled Release* **1987**, *5*, 37–42.
[52] N. A. Peppas, J. J. Sahlin, *Int. J. Pharm.* **1989**, *57*, 169–172.
[53] K. Giannousi, M. Menelaou, J. Arvanitidis, M. Angelakeris, A. Pantazaki, C. Dendrinou-Samara, *J. Mater. Chem. B* **2015**, *3*, 5341–5351.
[54] S. Sakat, A. Juvekar, M. Gambhire, *Int. J. Pharm. Pharm. Sci.* **2010**, *2*, 146–155.

Received: December 19, 2018

Nanoparticles for Drug Delivery

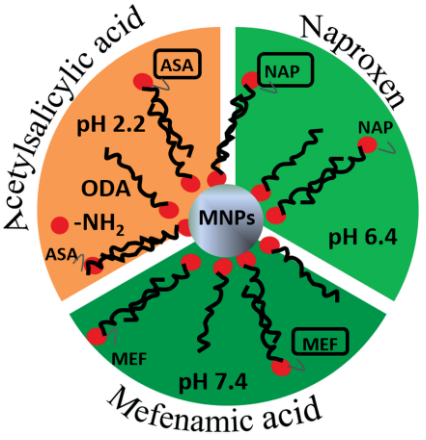

Magnetic nanoparticles (MNPs) functionalized with nonsteroidal anti-inflammatory drugs (NSAIDs) can be used for the combined diagnosis and treatment of inflammation-correlated diseases.

DOI: 10.1002/ejic.201801539